

Long-Pulse, High-Power Free-Electron Laser with No External Beam Focusing

J. A. Pasour, R. F. Lucey,^(a) and C. A. Kapetanakos

Plasma Physics Division, Naval Research Laboratory, Washington, D. C. 20375

(Received 23 July 1984)

We report the results of a free-electron laser experiment which has produced 1–2- μ sec duration pulses of ~ 30 -GHz radiation at power levels up to 4 MW. This is the first free-electron laser in the high-current operating regime to employ no external electron-focusing field. Consequently, there is no cyclotron emission, and the output radiation is unambiguously identified as free-electron laser emission.

PACS numbers: 42.55.-f

Currently, many laboratories in several countries around the world are investigating the free-electron-laser (FEL) mechanism.¹ This mechanism has the potential to lead to high-power, tunable, and efficient radiation sources that operate over a broad frequency range of the spectrum.

In this paper, we report results from a FEL experiment that has two novel features. First, there is not a guide magnetic field in the interaction region, although the electron current is relatively high, i.e., about 200 A. As a consequence of this feature, the cyclotron radiation that has plagued other experiments² is absent, and thus the FEL modes can be unambiguously identified and analyzed. Second, the duration of the beam pulse is 2 μ sec, i.e., about 40 times longer than in previous, high-beam-current FEL experiments. The long pulse duration of the present experiment can provide valuable information on the FEL saturation mechanism and other nonlinear effects.

Although our experiment is uniquely suited to operate in the oscillator mode, the results reported in this paper are from a superradiant amplifier experiment, and can be briefly summarized as follows: After propagating through the accelerator for ~ 3 m, the 700-keV, 2- μ sec-long electron pulse enters the interaction region. A helical magnetic wiggler drives the FEL and provides all the electron focusing. Since there is no cyclotron emission, the observed microwave output (4 MW at ~ 30 GHz) is unequivocally FEL emission. The radiation is tunable with beam energy as predicted. The duration of the microwave pulse is as long as 2 μ sec and its linewidth $\sim 10\%$. Finally, the shape of the radiation pulse suggests that saturation does not occur for at least 50% of the beam-pulse duration.

The electron beam is generated by a linear induction accelerator (LIA), which was designed and constructed at the National Bureau of Standards.³ Its unique feature is a 2- μ sec-duration pulse. The injector operates at 350–450 kV and incorporates an

Astron II electron gun.³ The cathode is located in an essentially null magnetic field ($B_z \leq 5$ G). A series of solenoidal coils is used to focus and transport the beam through the rest of the accelerator. Two accelerating gaps, driven by separate induction modules, are run at 100–150 kV, giving a final beam energy of 550 to 750 keV.

Although the electron gun was originally designed to operate with a thermionic cathode, the experiments described here have all been performed with a graphite-brush cathode.^{4,5} This 15-cm-diam, field-emission cathode is fabricated from 1-mm threads of 10- μ m graphite fibers. The threads are spaced 1 cm apart and extend 1 cm from the surface of an aluminum support plate. This cathode has proven to be very reliable, long-lived (thousands of pulses with no evidence of deterioration), and has greatly simplified the operation of the accelerator. The electron-gun voltage and current are constant to within 5% for 1.5 μ sec.⁵ The normalized beam emittance is $\approx 0.25\pi$ rad cm, which is only about twice the value measured with a thermionic cathode.

The wiggler is a bifilar helix having a 4-cm period and 4-cm diameter. The total wiggler length is 128 cm, including a 6-period adiabatic transition at each end. The inherently large field perturbation⁶ at the entrance end of the wiggler is reduced to $< 3\%$ of the peak field with an external compensating winding. The 3-cm-i.d., 0.75-mm-thick stainless-steel tube passing through the wiggler allows the pulsed wiggler field (100 μ s rise time) to penetrate nearly unperturbed to the axis.

One of the major advantages of the helical wiggler is that it provides radial focusing for the beam. This focusing is very evident in the experiment. As the beam enters the wiggler, it expands and its current decreases until it reaches the constant-amplitude portion of the wiggler. The current decrease in the transition region is a function of B_w , but if $B_w \geq 300$ G there is no discerni-

ble additional current loss through the constant-amplitude part of the wiggler. At the end of the wiggler, the beam is diverted to the wall of the beam tube.

Measurements of the beam position and size in the wiggler are performed with use of a sliding molybdenum target with an attached scintillator which is photographed from one end of the wiggler. The beam radius is typically ~ 0.5 cm, but the beam centroid is off axis as much as 0.5 cm. Consequently, the beam executes a spiral motion as it propagates through the wiggler.

The radiation is normally coupled out of the device through a conical horn and a 15-cm-diam Teflon vacuum window. The high-frequency output power is measured with a gas-breakdown spectrometer⁷ or with a calorimeter.⁸ The results agree within the accuracy of the diagnostics. The maximum radiated power is 4 MW and is obtained with $\epsilon_b = 700$ keV, $I_b = 200$ A, and $B_w = 625$ G.

There is a strong correlation between radiated power, beam current, and wiggler field. A sharp threshold is observed at $B_w \approx 400$ G for the generation of significant FEL radiation. Both the transported current and the microwave power peak at $B_w \sim 625$ –750 G. The ratio of radiated power to beam current is nearly constant from $B_w = 500$ G to 1 kG.

Theoretical output frequencies are given by the intersections of the waveguide-mode dispersion curve and the FEL-beam line, $\omega = v_z(k + k_w)$. For $\omega_b \ll \omega_{co}$, where ω_b is the beam plasma frequency

and ω_{co} is the cutoff frequency of a particular waveguide mode, it is easy to show

$$\omega = k_w v_z \gamma_z^2 \left\{ 1 \pm \beta_z \left[1 - \left(\frac{\omega_{co}}{k_w v_z \gamma_z} \right)^2 \right]^{1/2} \right\}, \quad (1)$$

where $k_w = 2\pi/\lambda_w$, λ_w is the wiggler period, v_z is the axial beam velocity, $\beta_z = v_z/c$, and $\gamma_z = (1 - \beta_z^2)^{-1/2}$. Normally, output is observed at both the high- and low-frequency intersections, but the low-frequency output is about an order of magnitude lower in power.

The frequency of the output radiation has been determined by use of a series of cutoff filters, a gas-breakdown spectrometer,⁷ and a Fabry-Perot interferometer. The measurements agree to within experimental accuracy. Two sets of Fabry-Perot data are shown in Fig. 1. Each point represents a single shot, and the dashed lines show the calibration curves at the two frequencies. The output frequency increases from 23 GHz to 31 GHz as the beam energy is increased from ~ 575 keV to ~ 650 keV. By comparing the width of the data peaks to that of the calibration peaks, we find the radiation linewidth is $\sim 10\%$. The fact that the Fabry-Perot output does not drop to as low a value as the calibration curves between peaks is consistent with the presence of an additional mode. Indeed, the high-pass-filter data indicate the presence of an additional broadband component (which cannot be resolved by the interferometer) with frequency from ~ 40 to 60 GHz.

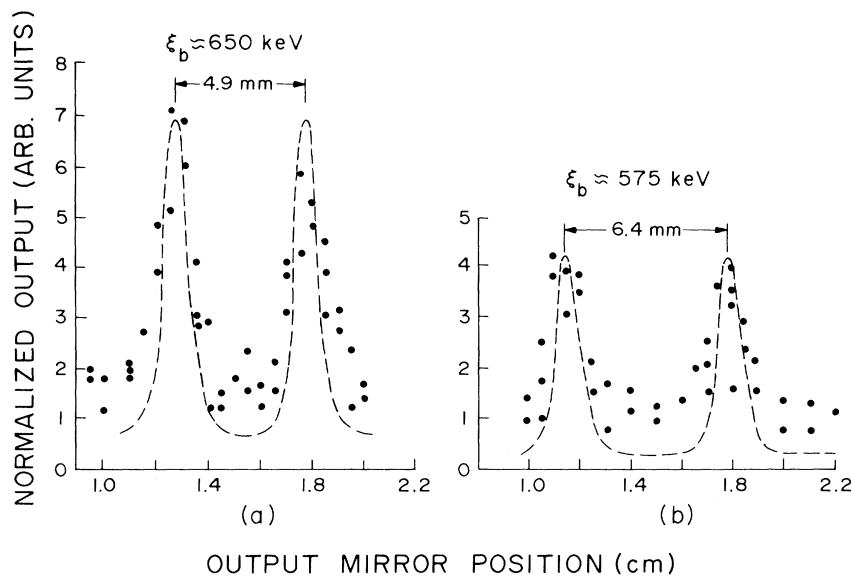


FIG. 1. Fabry-Perot interferometer data at two values of beam energy. Each point represents a single shot, and the dashed curves show the calibration at a single frequency.

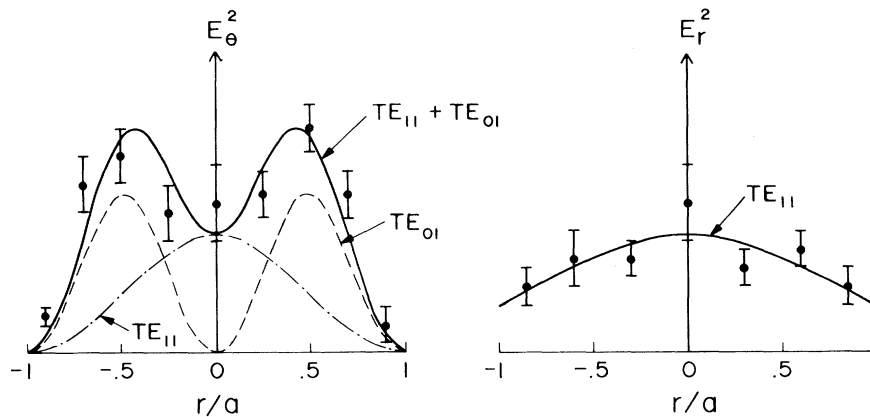


FIG. 2. Azimuthal and radial rf electric field variation along a diameter of the output horn. Also shown are the calculated profiles of the TE₁₁ and TE₀₁ modes.

To determine the radiation mode structure, a *Ka*-band pickup waveguide is placed at various positions on the face of the output window. The waveguide is rotated to detect either E_r or E_θ , the rf electric-field components. The results of these measurements are shown in Fig. 2. It can be seen that a good fit to the data is obtained by superimposing TE₁₁ and TE₀₁ modes of similar peak amplitudes. Both field components are essentially independent of θ , implying that the TE₁₁ mode is circularly polarized, as expected with the helical wiggler.

The 30–33 GHz radiation frequency that is measured when $B_w = 1$ kG and $\epsilon_b \approx 650$ keV is somewhat less than expected from Eq.(1). Figure 3 shows the predicted output frequencies for the TE₁₁ and TE₀₁ modes as a function of the calculated perpendicular velocity $\beta_\perp = eB_w/\gamma mck_w$. Note that a

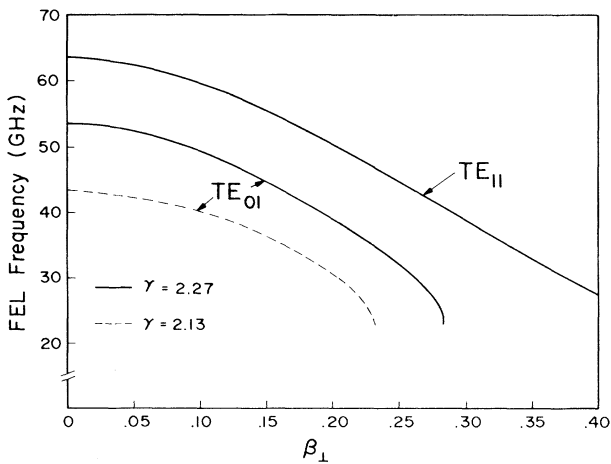


FIG. 3. FEL resonance frequency vs perpendicular electron velocity as calculated from Eq. (1).

β_\perp of 0.25 or 0.36 (corresponding to an effective wiggler field of 1.5 kG or 2.2 kG) would be required to generate 31 GHz radiation in the TE₀₁ or TE₁₁ mode, respectively, while the experimental parameters give $\beta_\perp = 0.16$. To a large degree, this apparent discrepancy can be explained by the observation that the beam centroid is ~ 0.5 cm off axis. The off-axis electrons experience a larger wiggler field and also undergo betatron oscillations, both of which increase β_\perp . For example, the outermost electrons are at $r = 1$ cm where the perpendicular field is calculated to be 76% higher than the field on axis. The TE₀₁ field-intensity profile is narrow and peaks at $r/a = 0.5$ ($r = 0.75$ cm), at which point the wiggler field enhancement is 39%. Thus, it is plausible that the electrons which couple to the TE₀₁ mode lie in a small annular region and have sufficiently large β_\perp and sufficiently small velocity spread to produce 31 GHz radiation with a 10% linewidth. The measured frequency of the broadband emission (~ 40 –60 GHz) is roughly consistent with the expected output frequencies in the TE₁₁ mode (which has a broad profile), given the axial velocity spread of the beam that results from the radial wiggler gradient.

The observed frequency tuning of the narrow-band output is also consistent with a TE₀₁ interaction, as shown in Fig. 3. With $\gamma = 2.13$, the largest β_\perp for which resonance can occur is $\beta_\perp = 0.23$, at which $f = 23$ GHz (the measured value). This value of β_\perp is consistent with that obtained in the $\gamma = 2.27$ case, with the assumption of the same reduction in axial velocity due to beam off-centering.

The peak power of 4 MW corresponds to an interaction efficiency of 3%. The theoretical cold-beam efficiency,⁹ $\eta = \omega_b/(\gamma^{1/2}\gamma_z ck_w)$, is $\eta \approx 10\%$.

It is unlikely that saturation has been reached in this single-pass, superradiant experiment, because the output power sometimes continues to increase up to $t = 1 \mu\text{sec}$. Therefore, given the beam-energy spread and the off-axis propagation of the beam through the wiggler, the observed efficiency is actually quite good.

Work is in progress to improve the beam quality and the beam centering in the wiggler. This should enhance the excitation of the TE_{11} mode, and increase the efficiency.¹⁰ The success of the experiment suggests that a repetitively pulsed, long-pulse, high-power FEL would be an attractive means of delivering high-energy millimeter-wavelength radiation. The long-pulse capability of this experiment also makes an oscillator configuration very attractive. We are currently addressing these issues.

We appreciate useful discussions during the course of this work with P. Sprangle, C. M. Tang, and C. W. Roberson. We also thank S. Gold for the use of the microwave calorimeter and J. Walsh for the design of the Fabry-Perot interferometer. This work was supported by the Office of Naval Research.

^(a)Permanent address: Pulse Sciences Inc., San Leandro, Cal. 94577.

¹*Free Electron Generators of Coherent Radiation*, edited by C. A. Brau, S. F. Jacobs, and M. O. Scully, SPIE Conference Proceedings Vol. 453 (SPIE, Bellingham, Wash., 1984).

²R. E. Shefer and G. Bekefi, in *Physics of Quantum Electronics: Free Electron Generators of Coherent Radiation*, edited by S. Jacobs, H. Polloff, M. Scully, G. Moore, M. M. Sargent, III, and R. Spitzer (Addison-Wesley, Reading, Mass., 1982), Vol. 9, p. 703.

³J. E. Leiss, N. J. Norris, and M. A. Wilson, *Part. Accel.* **10**, 223 (1980).

⁴J. J. Ramirez and D. L. Cook, *J. Appl. Phys.* **51**, 4602 (1980).

⁵J. A. Pasour, R. F. Lucey, and C. W. Roberson, in *Free Electron Generators of Coherent Radiation*, edited by C. A. Brau, S. F. Jacobs, and M. O. Scully, SPIE Conference Proceedings Vol. 453 (SPIE, Bellingham, Wash., 1984), pp. 328–335.

⁶J. Fajans, *J. Appl. Phys.* **55**, 43 (1984).

⁷F. Mako, J. A. Pasour, C. W. Roberson, and R. Lucey, *Rev. Sci. Instrum.* **55**, 712 (1984).

⁸R. H. Jackson, S. H. Gold, R. K. Parker, H. P. Freund, P. C. Efthimion, V. L. Granatstein, M. Herndon, A. Kinkead, J. Kosakowski, and T. Kwan, *J. Quantum Electron.* **19**, 346 (1983).

⁹P. Sprangle, R. A. Smith, and V. L. Granatstein, in *Infrared and Millimeter Waves: Sources of Radiation Vol. 1*, edited by K. J. Button (Academic, New York, 1979), pp. 279–329.

¹⁰J. Fajans, G. Bekefi, Y. Z. Yin, and B. Lax, *Phys. Rev. Lett.* **53**, 246 (1984).